Article

Cell Host & Microbe

miR-122 Stimulates Hepatitis C Virus RNA Synthesis by Altering the Balance of Viral RNAs Engaged in Replication versus Translation

Graphical Abstract

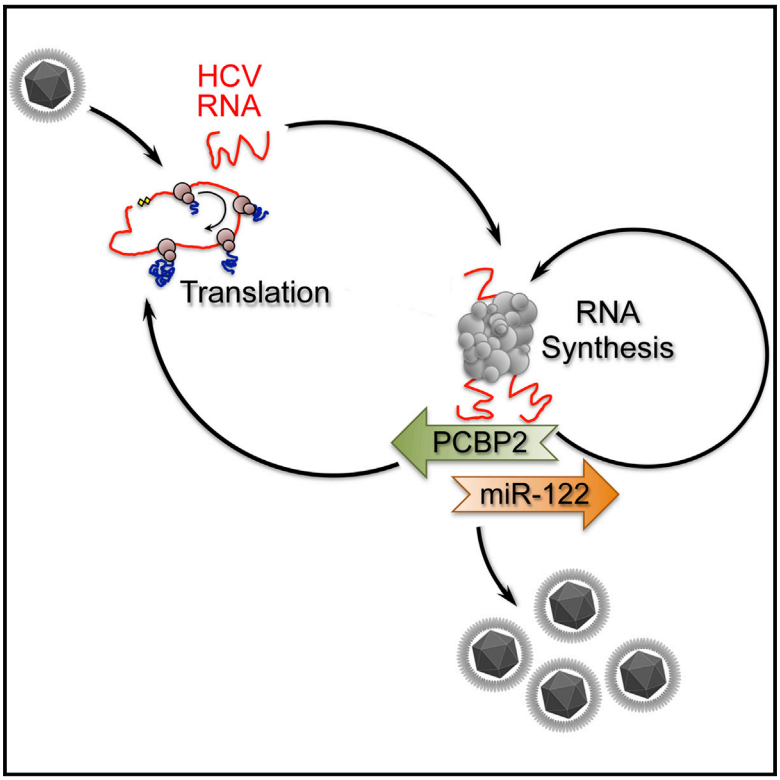

Authors

Takahiro Masaki, Kyle C. Arend, ...,
Nathaniel J. Moorman,
Stanley M. Lemon

Correspondence

smlemon@med.unc.edu

In Brief

miR-122 is an important host factor for HCV, acting in part by protecting its genome from Xrn1-mediated decay. Masaki et al. show miR-122 also directly stimulates viral RNA synthesis by competing with PCBP2 for binding to the RNA and increasing the fraction of viral RNAs engaged in replication versus translation.

Highlights

- miR-122 promotes HCV replication independently of protecting HCV RNA from Xrn1
- miR-122 stimulates HCV RNA synthesis prior to promoting viral protein synthesis
- Stimulation of RNA synthesis requires active protein translation, AGO2, and PCBP2
- miR-122 displaces PCBP2 to rebalance RNA engagement in RNA versus protein synthesis

Masaki et al., 2015, Cell Host & Microbe *17*, 217–228
February 11, 2015
http://dx.doi.org/10.1016/j.chom.2014.12.014

CellPress

Cell Host & Microbe
Article

miR-122 Stimulates Hepatitis C Virus RNA Synthesis by Altering the Balance of Viral RNAs Engaged in Replication versus Translation

Takahiro Masaki,[1,4] Kyle C. Arend,[2] You Li,[1] Daisuke Yamane,[1] David R. McGivern,[1,3] Takanobu Kato,[4] Takaji Wakita,[4] Nathaniel J. Moorman,[1,2] and Stanley M. Lemon[1,2,3,*]
[1]Lineberger Comprehensive Cancer Center
[2]Department of Microbiology & Immunology
[3]Division of Infectious Diseases, Department of Medicine
University of North Carolina at Chapel Hill, Chapel Hill, NC 27517, USA
[4]Department of Virology II, National Institute of Infectious Diseases, Toyama 1-23-1, Shinjuku-ku, Tokyo 162-8640, Japan
*Correspondence: smlemon@med.unc.edu
http://dx.doi.org/10.1016/j.chom.2014.12.014

SUMMARY

The liver-specific microRNA, miR-122, stabilizes hepatitis C virus (HCV) RNA genomes by recruiting host argonaute 2 (AGO2) to the 5′ end and preventing decay mediated by exonuclease Xrn1. However, HCV replication requires miR-122 in Xrn1-depleted cells, indicating additional functions. We show that miR-122 enhances HCV RNA levels by altering the fraction of HCV genomes available for RNA synthesis. Exogenous miR-122 increases viral RNA and protein levels in Xrn1-depleted cells, with enhanced RNA synthesis occurring before heightened protein synthesis. Inhibiting protein translation with puromycin blocks miR-122-mediated increases in RNA synthesis, but independently enhances RNA synthesis by releasing ribosomes from viral genomes. Additionally, miR-122 reduces the fraction of viral genomes engaged in protein translation. Depleting AGO2 or PCBP2, which binds HCV RNA in competition with miR-122 and promotes translation, eliminates miR-122 stimulation of RNA synthesis. Thus, by displacing PCBP2, miR-122 reduces HCV genomes engaged in translation while increasing the fraction available for RNA synthesis.

INTRODUCTION

Hepatitis C virus (HCV) is an important human pathogen that infects as many as 185 million persons worldwide, causing end-stage liver disease and hepatocellular carcinoma (Thomas, 2013). Classified within the family *Flaviviridae*, it possesses an uncapped, positive-sense, single-stranded RNA genome with structured 5′ and 3′ untranslated regions (UTRs) flanking a large open reading frame that encodes a polyprotein that is processed into ten viral proteins (Scheel and Rice, 2013). The 5′ UTR contains an internal ribosome entry site (IRES) that mediates cap-independent initiation of viral protein synthesis and, at its extreme 5′ end, RNA signals essential for genome replication (Friebe et al., 2001; Honda et al., 1999). The 5′ UTR serves as a platform for recruitment of cellular factors that are essential for viral translation and/or RNA replication, including, among others, poly(rC)-binding protein 2 (PCBP2), eukaryotic initiation factor 3 (eIF3), and microRNA 122 (miR-122) (Fukushi et al., 2001; Jopling et al., 2005; Kieft et al., 2001; Pestova et al., 1998; Wang et al., 2011).

miR-122 is a highly expressed and liver-specific small RNA that accounts for a large fraction of miRNAs in hepatocytes (Chang et al., 2004). It regulates expression of numerous liver-specific genes post-transcriptionally by binding to the 3′ UTR of cellular mRNAs (Chang et al., 2004; Lanford et al., 2010). In contrast to this typical miRNA action, miR-122 binds to two conserved sites (S1 and S2) near the 5′ end of the HCV 5′ UTR and stimulates replication of the virus (Jangra et al., 2010; Jopling et al., 2005, 2008). Mutations introduced into the S1 and S2 sites that disrupt miR-122 binding severely impair replication (Jangra et al., 2010; Jopling et al., 2005; Norman and Sarnow, 2010). However, S1 and S2 virus mutants can be rescued by transfection of modified miR-122 oligonucleotides containing complementary mutations that restore binding to the 5′ UTR, indicating that miR-122 promotes HCV replication directly and not indirectly by modulating host gene expression. Silencing miR-122 by administration of a complementary locked nucleic acid (LNA) oligomer has shown therapeutic promise in preclinical and clinical studies (Janssen et al., 2013; Lanford et al., 2010), highlighting the importance of miR-122 in the virus life cycle.

Although well established, an understanding of how miR-122 promotes HCV replication has remained elusive. Early studies suggested that it might act, in part, by stimulating IRES-directed translation (Henke et al., 2008). Later work supports this view (Jangra et al., 2010; Roberts et al., 2011; Zhang et al., 2012), but recent data suggest that increases in viral protein expression may result from an unusual stabilizing effect of miR-122 on the HCV genome (Shimakami et al., 2012a). miR-122 recruits argonaute 2 (AGO2) protein to the 5′ end of the viral RNA (Conrad et al., 2013; Shimakami et al., 2012a) and protects the genome from 5′ decay mediated by the cytoplasmic 5′ exonuclease, Xrn1 (Li et al., 2013b). miR-122 and Xrn1 thus have competing effects on the stability and rate of decay of HCV RNA in infected

cells, and Xrn1 depletion enhances both viral RNA abundance and the production of infectious virus in cell culture (Li et al., 2013b). However, while miR-122 has no effect on the stability of HCV RNA in Xrn1-depleted cells due to the absence of 5′ exonuclease activity, supplementing such cells with exogenous miR-122 continues to boost HCV replication (Li et al., 2013b). Furthermore, Xrn1 depletion does not rescue replication of a viral mutant that is defective in miR-122 binding (Li et al., 2013b). These results indicate that miR-122 has an additional key function in the HCV replication cycle above and beyond its ability to physically stabilize the genome (Li et al., 2013a). Consistent with this, some miR-122 mutants protect RNA against Xrn1-mediated decay, yet fail to promote virus replication (Mortimer and Doudna, 2013).

Here, we demonstrate the direct involvement of miR-122 in viral RNA synthesis. We show that augmenting endogenous miR-122 abundance stimulates viral RNA synthesis under conditions of Xrn1 depletion in which miR-122 has no effect on viral RNA stability. While we find translation and replication of the viral RNA are tightly coupled processes, miR-122-mediated increases in RNA synthesis temporally precede increases in viral protein synthesis. Surprisingly, however, miR-122 does not stimulate viral RNA synthesis in the absence of active protein translation or following RNAi-mediated depletion of PCBP2. Our results indicate that the primary function of miR-122 is to enhance HCV RNA synthesis, and suggest a mechanism by which miR-122 alters the balance of viral genomes engaged in genome synthesis versus protein translation.

RESULTS

miR-122 Supplementation Exerts a Primary Effect on Viral RNA Synthesis

Although the positive influence of miR-122 on HCV genome amplification is well known, it remains unclear whether its primary effect is on viral protein or viral RNA synthesis, two critical steps in the viral life cycle. We thus compared the kinetics of miR-122-mediated increases in the abundance of viral RNA and viral proteins in HCV-infected cells in an effort to determine whether one precedes the other and thus might represent a primary effect of miR-122. We supplemented the endogenous abundance of miR-122 in HJ3–5 virus-infected cells by transfecting synthetic duplex miR-122 or, as a control, a brain-specific miRNA, miR-124 (see Experimental Procedures). Because miR-122 stabilizes genomic RNA by protecting it from Xrn1-mediated decay (Li et al., 2013b), we examined the kinetics of HCV RNA and protein accumulation both with and without prior siRNA-mediated depletion of Xrn1 (Figure 1A). Xrn2, a predominantly nuclear 5′ exonuclease, has also been suggested to mediate HCV RNA decay (Sedano and Sarnow, 2014). However, we found that Xrn2 depletion has no effect on the decay of HJ3–5 RNA, whereas Xrn1 depletion significantly slows it (Figures S1A–S1D). Moreover, we confirmed that miR-122 supplementation has only a minimal, non-significant effect on RNA decay in Xrn1-depleted cells (Figures S1E and S1F) (Li et al., 2013b). Nonetheless, miR-122 supplementation mediated significant increases in viral RNA abundance and NS5A protein expression in both Xrn1-depleted cells as well as in cells transfected with a non-targeting siRNA, siCtrl (Li et al., 2013b) (Figure 1). As expected (Li et al., 2013b), these increases were greater in siCtrl- than in siXrn1-transfected cells (Figure 1). In multiple experiments, increases in viral RNA and NS5A abundance occurred with a similar kinetic and were significant within 6–9 hr following transfection of miR-122 (Figures 1C and 1E). These results demonstrate very close coupling between increases in viral RNA synthesis and protein expression, but do not reveal which is the primary target of miR-122.

Given this tight coupling between viral RNA and protein synthesis, we developed methods to measure these processes directly by metabolic labeling (Figure 2A). After confirming Xrn1 depletion (Figure 2B), cells were labeled with either 5-ethynyl uridine (EU) or [^{35}S]-methionine/cysteine following transfection with miR-122 or the control miR-124. Nascent viral RNA was measured by qRT-PCR following pull-down of biotin-conjugated, EU-labeled RNA (see Experimental Procedures). We used HJ3–5/NS5A^{YFP} virus for these experiments as it expresses NS5A with an internal yellow fluorescent protein (YFP) fusion, allowing measurement of nascent protein synthesis by immunoprecipitation of [^{35}S]-labeled NS5A-YFP with anti-YFP antibody followed by SDS-PAGE and phosphorimager analysis (Figure 2C). Remarkably, we observed a reproducible increase in nascent viral RNA synthesis within 1 hr in cells transfected with miR-122 versus miR-124, whereas there was no measurable increase (and in fact a slight, but significant, decrease) in NS5A-YFP synthesis during this period (Figure 2D; $p < 0.01$ by two-sided Mann-Whitney test). Increased NS5A-YFP synthesis was observed at later time points, likely because of increases in viral RNA available for translation. Since the $t_{1/2}$ of replicating HJ3–5 RNA is approximately 8.3–9.6 hr in Xrn1-depleted cells (Figure S1F), the increase in viral RNA synthesis at 1 hr cannot be explained by enhanced RNA stability. Moreover, while miR-122 appeared to protect newly synthesized RNA from degradation, this effect was not observed in Xrn1-depleted cells (Figure S2). Collectively, these data provide strong evidence that miR-122 directly promotes HCV RNA synthesis, and confirm close coupling between viral RNA and protein synthesis.

AGO2 is recruited to the 5′ end of HCV RNA by miR-122, and required for miR-122-mediated stabilization of HCV RNA and amplification of viral RNA abundance (Conrad et al., 2013; Shimakami et al., 2012a). To determine whether AGO2 is also required for miR-122 stimulation of viral RNA synthesis, we transfected cells with AGO2-specific siRNA prior to miR-122 supplementation (Figure 2E). Consistent with our earlier findings (Shimakami et al., 2012a), viral RNA synthesis was significantly reduced in AGO2-depleted cells compared with cells transfected with control siRNA (Figure 2F; $p < 0.01$). More importantly, in contrast to the results shown in Figure 2D, there was no increase in viral RNA synthesis during the first hour after miR-122 transfection (Figure 2F). Thus, miR-122 stimulates RNA synthesis in an AGO2-dependent fashion.

miR-122 Sequestration and Viral RNA Synthesis

Next, we considered whether sequestering miR-122 by transfecting a complementary LNA antagomir of miR-122 would have an effect opposite to miR-122 supplementation, reducing HCV RNA synthesis in short-term experiments. Given that the regulation of RNA synthesis by miR-122 requires AGO2 (Figure 2F), we first compared the kinetics with which miR-122

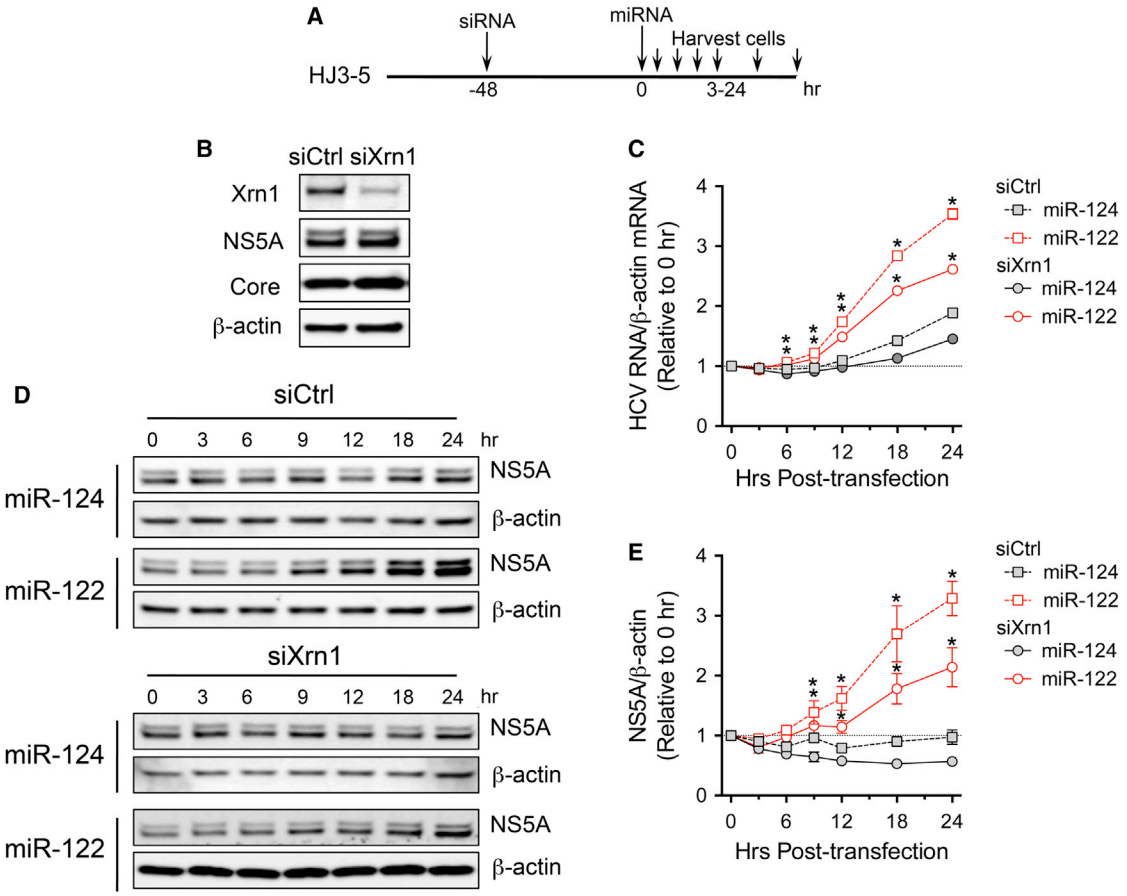

Figure 1. Kinetics of miR-122-Mediated Increases in RNA and Protein Abundance

(A) Experimental design; HJ3–5 virus-infected cells were transfected with scrambled control (siCtrl) or Xrn1-specific (siXrn1) siRNA and 2 days later re-transfected with duplex miRNAs (0 hr), then harvested at the times indicated for assays of HCV RNA and NS5A protein.

(B) Immunoblots of Xrn1, NS5A, and core protein at 0 hr. β-actin was a loading control.

(C) HCV RNA abundance in cells transfected with siCtrl or siXrn1 and supplemented with miR-122 or miR-124. RNA was quantified by qRT-PCR relative to β-actin mRNA.

(D) Immunoblots of NS5A protein in cells transfected with (top panels) siCtrl or (bottom panels) siXrn1 following miR-124 or miR-122 supplementation.

(E) NS5A expression was quantified based on infrared fluorescence intensities in immunoblots shown in (D) relative to β-actin expression. Results shown in (C) and (E) represent mean fold change ± SEM from 0 hr in triplicate cultures and are representative of multiple independent experiments. *$p < 0.05$ (miR-122 versus miR-124) by two-way ANOVA with correction for multiple comparisons. miR-122-mediated increases in RNA and NS5A protein were greater in siCtrl-transfected cells than Xrn1-transfected cells at 18 and 24 hr ($p < 0.05$). See also Figure S1.

supplementation and sequestration modulate loading of the miRNA into AGO2. AGO2 pull-down followed by qRT-PCR quantitation of co-immunoprecipitated miR-122 revealed that transfection of miR-122 resulted in a 5- to 10-fold increase in AGO2-bound miR-122 within 1 hr (Figure 3A). In contrast, transfection of anti-miR-122 reduced the abundance of miR-122 bound to AGO2 by only 30% after 1 hr, and 90% only after 12 hr (Figure 3B).

In keeping with the slow kinetic with which sequestration reduces AGO2-bound miR-122, neither viral RNA nor NS5A-YFP synthesis was reduced 0–1 or 3–6 hr after transfection of the anti-miR-122 LNA (Figures 3C and 3D). However, both were significantly reduced by 6–12 hr post-transfection ($p = 0.03$ for NS5A-YFP, and $p < 0.001$ for HCV RNA, compared with cells transfected with an anti-random control). Consistent with miR-122 exerting its primary effect on viral RNA synthesis, the reduction in nascent RNA was significantly greater than in nascent NS5A-YFP (64% ± 6.9% SEM of anti-random control for RNA versus 86% ± 5.6% for NS5A-YFP, $p < 0.001$).

miR-122 Does Not Stimulate Viral Translation

To directly assess how the abundance of miR-122 influences HCV protein translation in the absence of ongoing viral RNA synthesis, we treated stably infected cells with potent inhibitors of the NS5B RNA-dependent RNA polymerase (Figure 4A). After achieving high-level depletion of Xrn1 (Figure 4B), cells were treated with PSI-6130 or sofosbuvir (SOF) for 14 hr, then transfected with duplex miR-122 or miR-124 and HCV RNA and NS5A-YFP synthesis quantified as described above. HCV RNA synthesis was reduced to background levels by the NS5B inhibitors (Figure 4C, left), supporting the specificity of this assay. Total HCV RNA was reduced, but still abundant, in the cells

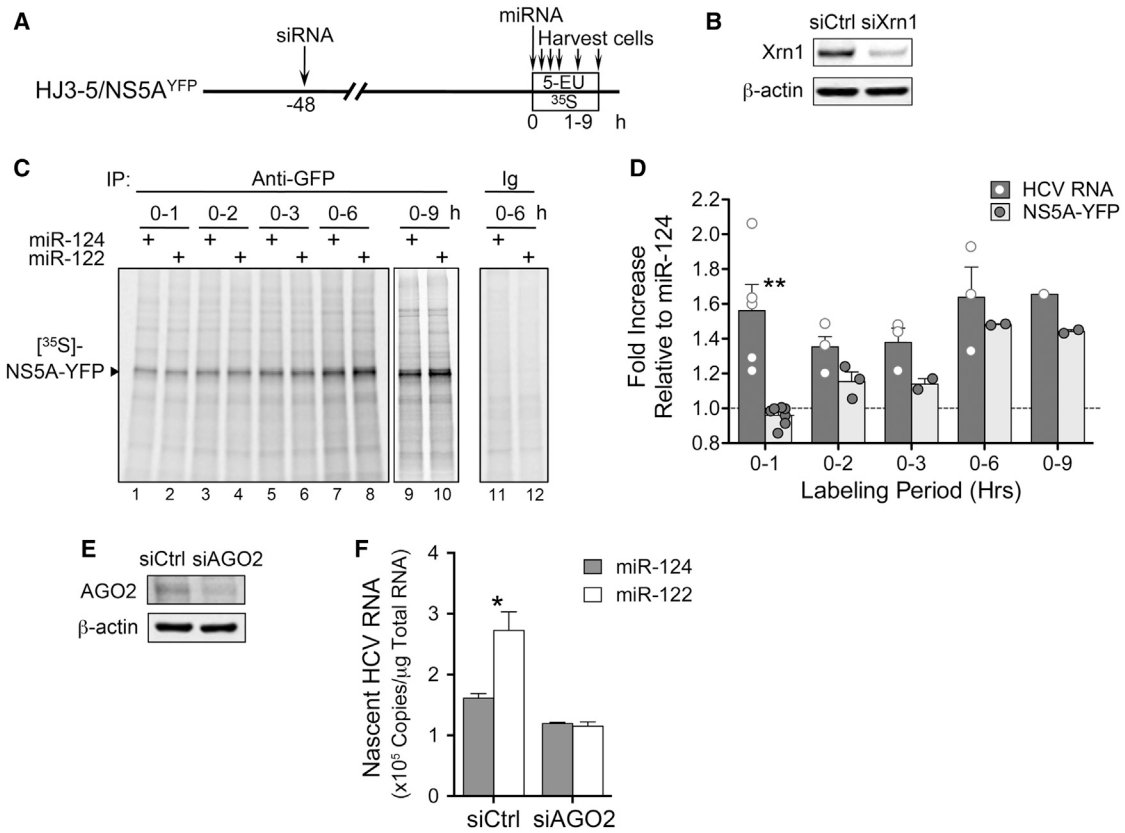

Figure 2. miR-122 Directly Stimulates Nascent HCV RNA Synthesis

(A) Experimental design; HJ3–5/NS5A^{YFP} virus-infected cells were transfected with siRNAs, then 2 days later, re-transfected with duplex miRNAs (0 hr) and immediately fed with media containing 5-EU or [^{35}S]-methionine/cysteine. Cells were harvested at intervals for quantitation of nascent HCV RNA and NS5A-YFP as described in Experimental Procedures.

(B) Immunoblot of Xrn1 at the time of miRNA transfection from a representative experiment. β-actin is a loading control.

(C) Metabolically labeled [^{35}S]-NS5A-YFP from a representative experiment. Cell lysates were immunoprecipitated with rabbit anti-GFP antibody (Anti-GFP, lanes 1–10) or with an isotype control (Ig, lanes 11 and 12). Immunoprecipitates were separated by SDS-PAGE, and labeled proteins visualized by phosphorimager analysis. The labeling period (0–1 to 0–9 hr) is indicated near the top.

(D) Increases in 5-EU-labeled HCV RNA and [^{35}S]-NS5A-YFP synthesis following miR-122 supplementation. 5-EU-labeled HCV RNA was precipitated and quantified by qRT-PCR. [^{35}S]-NS5A-YFP was quantified by phosphorimager analysis of SDS-PAGE gels. Results for both 5-EU-labeled HCV RNA and [^{35}S]-NS5A-YFP are shown as bars representing the mean fold increase ± SEM in cells supplemented with miR-122 relative to cells supplemented with the control miR-124 for labeling periods ranging from 0–1 to 0–9 hr post-transfection. Individual results from replicate independent experiments are plotted as empty (HCV RNA) or full (NS5A-YFP) symbols. **$p < 0.01$ by two-sided Mann-Whitney test.

(E) Immunoblot showing AGO2 abundance in cells transfected 96 and 48 hr previously with siAGO2 or siCtrl.

(F) Impact of miR-122 supplementation on nascent HCV RNA in cells depleted of AGO2. The 5-EU labeling period was from 0 to 1 hr following transfection of miR-124 or miR-122. Results shown represent the mean ± SEM from triplicate cultures and are representative of multiple independent experiments. *$p < 0.05$ by two-sided t test. See also Figure S2.

(~5 × 10^7 copies/μg total RNA) at the end of the 12-hr labeling period (Figure 4C, right), and there was no difference in its abundance in cells supplemented with miR-122 versus those transfected with miR-124. This further confirms that miR-122 does not have a stabilizing effect on HCV RNA in Xrn-1 depleted cells (Li et al., 2013b). The amount of newly synthesized [^{35}S]-labeled NS5A-YFP protein was also reduced by the polymerase inhibitors due to the reduction in RNA template available for translation (Figure 4D). Most importantly, however, miR-122 supplementation caused only marginal, non-significant increases in NS5A-YFP synthesis in the PSI-6130- and SOF-treated cells (Figure 4E). These data are in agreement with a primary effect of miR-122 on HCV RNA synthesis, and not viral protein translation.

miR-122 Stimulation of Viral RNA Synthesis Requires Active Protein Translation

While translation of an incoming positive-strand RNA virus genome is necessary to establish replication complexes and initiate viral RNA synthesis in newly infected cells, prior studies indicate that continued protein translation is not required for ongoing HCV or flaviviral RNA synthesis (Shi et al., 2003; Westaway et al., 1999). This suggests that essential replicase components are either recycled for new rounds of viral RNA synthesis, or are present in excess abundance. To determine whether miR-122 would induce increases in RNA synthesis in the absence of ongoing translation, we treated infected Xrn1-depleted cells with puromycin or cycloheximide (CHX) (Figures 5A and 5B). Both

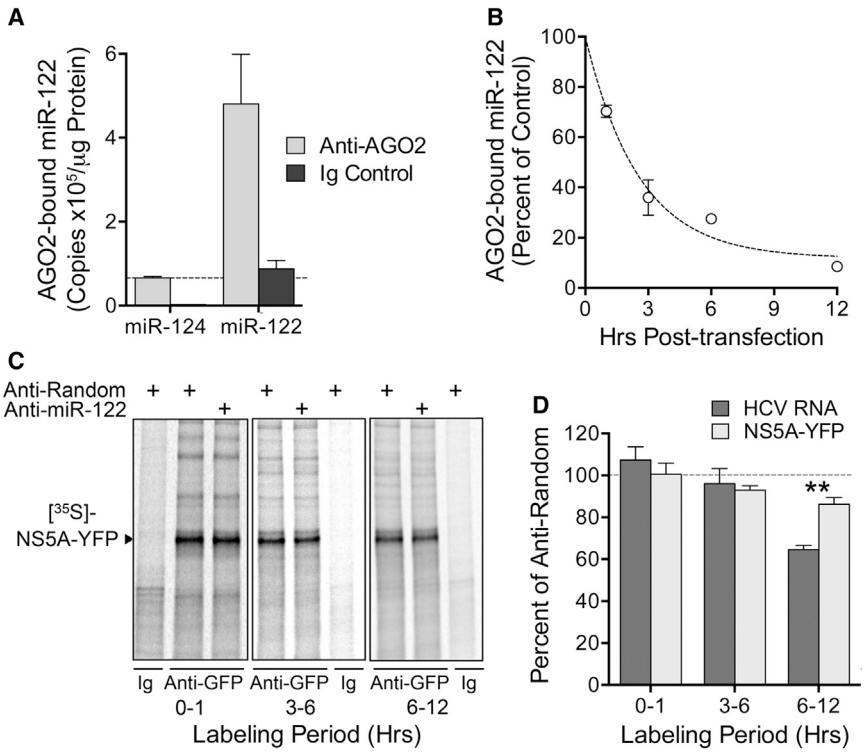

Figure 3. miR-122 Sequestration and Viral RNA Synthesis

(A) qRT-PCR quantitation of miR-122 co-immunoprecipitating with AGO2 in cell lysates prepared 1 hr after transfection of miR-122 (supplementation) or miR-124 (control). Shown are the mean ± SEM miR-122 copies per μg total protein (used for immunoprecipitation) precipitated with anti-AGO2 versus an irrelevant immunoglobulin (Ig) from two independent experiments.

(B) AGO2-bound miR-122 abundance at various intervals following transfection of the miR-122-specific LNA antagomir (sequestration). Results are shown as the mean ± SEM percent AGO2-bound miRNA in cells transfected with anti-random control.

(C) Nascent [^{35}S]-NS5A-YFP recovered from HJ3–5/NS5A^{YFP} virus-infected cells labeled 0–1, 3–6, or 6–12 hr following transfection of the anti-miR-122 antagomir or anti-random. Xrn1-depleted cells were used in experiments involving labeling periods beyond 1 hr. See legend to Figure 2C for details.

(D) Reductions in nascent 5-EU-labeled HCV RNA and [^{35}S]-NS5A-YFP following miR-122 sequestration. Results are shown as the mean percent ± SEM compared with cells transfected with anti-random (n = 3–6). Labeling periods were 0–1, 3–6, and 6–12 hr post-transfection, as in (C). **$p < 0.01$ by two-sided Mann-Whitney test.

inhibitors caused a complete or near-complete inhibition of viral and cellular protein synthesis without a noticeable effect on total cellular protein abundance over the 5 hr course of the experiment (Figure 5C). Surprisingly, short-term treatment (3–5 hr) with puromycin increased nascent viral RNA synthesis as much as or more than miR-122 supplementation in the absence of puromycin (Figure 5D). In contrast, there was no increase in nascent viral RNA synthesis after 4-hr treatment with CHX (Figure 5E). This difference is likely due to puromycin-induced dissociation of translating ribosomes from viral RNA, as this would lead to increased availability of viral RNA templates for RNA synthesis as observed in vitro with poliovirus (Barton et al., 1999). In contrast, CHX freezes ribosomes and prevents their clearance from RNA.

Even more surprising, however, miR-122 supplementation had no effect on nascent viral RNA synthesis in cells treated with either puromycin or CHX (Figures 5D and 5E). The lack of miR-122 stimulation of RNA synthesis was not related to insufficient AGO2, as AGO2 abundance was minimally reduced after 5 hr of translational shutoff (Figures S3A and S3B). Moreover, although reduced from untreated cells, miR-122 supplementation substantially increased the quantity of miR-122 that co-immunoprecipitated with AGO2 from lysates of puromycin-treated cells (Figure S3C). Lengthier shutdown of protein synthesis (12–15 hr), exceeding the estimated half-lives of nonstructural HCV proteins (Pietschmann et al., 2001), significantly decreased viral RNA synthesis in Xrn1-depleted cells and similarly eliminated any enhancement of nascent viral RNA synthesis by miR-122 (Figure S4). Collectively, these results confirm earlier reports that continuing protein translation is not required for HCV RNA synthesis as long as there is a sufficient abundance of the requisite nonstructural proteins (Shi et al., 2003; Westaway et al., 1999). In contrast, active protein translation is required for miR-122 to stimulate HCV RNA synthesis.

miR-122 Rebalances RNA Engagement in Translation versus RNA Synthesis

Since puromycin treatment and miR-122 supplementation caused similar, non-additive increases in HCV RNA synthesis (Figure 5D), we considered the possibility of a common underlying mechanism. Puromycin increases poliovirus RNA synthesis in cell-free replication reactions by clearing ribosomes from viral RNA, thereby providing more template for RNA synthesis (Barton et al., 1999). A partial inhibition of HCV translation initiation by miR-122 could have a similar impact on viral RNA synthesis. To assess this possibility, we analyzed the distribution of HCV RNA in rate-zonal gradients loaded with polysomes isolated from infected cells 1–2 hr after transfection with miR-122 or the control miR-124 (Figures 6 and S5). As anticipated, miR-122 induced a decrease in the proportion of HCV RNA associating with polysomes engaged in translation (Figure 6A, fractions 11–13) and an increase in less translationally active RNA co-sedimenting with 80S ribosomes (fractions 7–9) (Figure 6A). These changes were less than those observed with puromycin (Figure 6B), but they were reproducible and statistically significant ($p < 0.005$). In contrast, no changes were evident in β-actin mRNA distribution. Substantially smaller changes occurred in the distribution of chloride intracellular channel 4 (CLIC4) and cationic amino acid transporter 1 (CAT1) mRNAs within an hour of transfecting miR-122, both natural targets of the miRNA (Figure 6C). We conclude from these results that miR-122 induces an immediate rebalancing of the proportion of viral RNA engaged in translation versus that templating new viral RNA

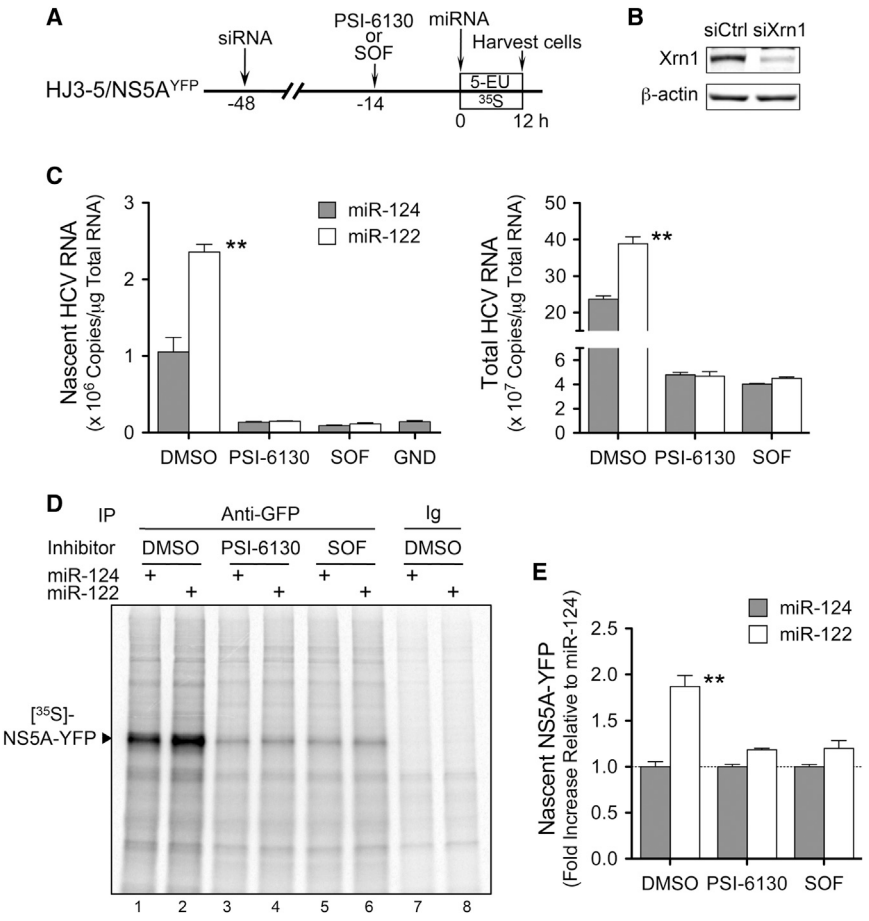

Figure 4. miR-122 and Viral Translation following Arrest of HCV RNA Synthesis

(A) Experimental design; Huh-7 cells that were stably infected with HJ3–5/NS5A^{YFP} virus (see Experimental Procedures) were transfected with siRNAs and then treated with 50 μM of PSI-6130 or 10 μM of sofosbuvir (SOF) for 14 hr before transfection of duplex miR-124 or miR-122 (0 hr). After miRNA transfection, cells were incubated in fresh culture media containing [^{35}S]-methionine/cysteine or 5-EU plus PSI-6130 or SOF for an additional 12 hr before being harvested for assay of nascent HCV RNA and NS5A-YFP.

(B) Immunoblot of Xrn1 60 hr following siRNA transfection. β-actin is a loading control.

(C) Left: nascent HCV RNA synthesis in cells transfected with miR-122 or miR-124 following treatment with the NS5B inhibitors. "GND" cells were electroporated with 10 μg of replication-defective HJ3–5 NS5B/GND RNA 7 days prior to the experiment. They contain no replication-competent HCV RNA, and thus allow assessment of background activity in the nascent RNA synthesis assay. Results shown are means ± SEM from triplicate cultures and are representative of multiple independent experiments. Right: total HCV RNA abundance at the end of the 12-hr labeling period.

(D) NS5A-YFP synthesis following arrest of viral RNA synthesis. Lysates of cells labeled with [^{35}S]-methionine/cysteine as in (A) were immunoprecipitated with anti-GFP or isotype control (Ig) antibody, and precipitates separated by SDS-PAGE. [^{35}S]-labeled NS5A-YFP was visualized with a phosphorimager.

(E) Phosphorimager quantitation of the effect of miR-122 supplementation on labeled NS5A-YFP protein in cells in which HCV RNA synthesis was arrested with NS5B inhibitors. Results are shown as the fold increase in NS5A-YFP synthesis in miR-122-versus miR-124-transfected cells, and are the mean ± SEM from triplicate cultures in a representative experiment. For all panels, **$p < 0.01$ by two-way ANOVA.

synthesis. By 2 hr, the increase in newly synthesized RNA results in a net increase in viral protein synthesis (Figure 2D), although the redistribution of HCV RNA persists (Figure S6).

miR-122 Stimulation of Viral RNA Synthesis Is PCBP2 Dependent

In addition to miR-122/AGO2, several cellular proteins, including the heterogeneous nuclear ribonuclear proteins PCBP2 (hnRNP E2) and hnRNP L, bind to the 5′ end of the HCV genome and facilitate its replication (Fukushi et al., 2001; Li et al., 2014; Wang et al., 2011). PCBP2 is of particular interest, as it regulates the IRES-initiated translation of poliovirus, another positive-strand RNA virus, and facilitates both circularization and translation of the HCV genome (Perera et al., 2007; Wang et al., 2011). Recent studies in our laboratory also show that PCBP2 competes with miR-122 for binding to synthetic RNA representing the 5′ 47 nts of HCV (Li et al., 2014) (Figure 7A). In similar pull-down experiments, we found that a two-base change (nts 41–42) within the S2 binding site of miR-122 ablated PCBP2, but not hnRNP L, binding (Figure 7B). This confirms that a major PCBP2 binding site overlaps one of the two functional miR-122 binding sites, suggesting in turn that miR-122 might skew the engagement of viral RNA molecules away from translation toward RNA synthesis by competing with and displacing PCBP2. Were this the case, we reasoned that miR-122 supplementation would have little if any positive effect on HCV RNA synthesis in cells depleted of PCBP2. To test this hypothesis, we depleted stably infected cells of PCBP2 by two successive transfections of PCBP2-specific siRNA (Figures 7C and 7D). This resulted in modest reductions in NS5A-YFP and HCV RNA abundance 48 hr after the second siRNA transfection (83% ± 7% and 80% ± 4% of siCtrl-transfected cells, $p = 0.12$ and $p < 0.01$, respectively) (Figures 7D and 7E). After transfecting the cells with miR-124 or miR-122, we assessed nascent NS5A-YFP and HCV RNA synthesis using the methods described above. In cells supplemented with the control miRNA, miR-124, prior PCBP2 depletion reduced NS5A-YFP synthesis to 82% ± 2% of that in control cells (Figures 7F and 7G; $p < 0.001$). In contrast, there was no reduction in viral RNA synthesis (103% ± 4%) (Figure 7H). This suggests that PCBP2 depletion either increased the efficiency of RNA synthesis or proportion of HCV RNAs engaged in viral RNA synthesis. Furthermore, as anticipated, miR-122 supplementation did not stimulate either viral protein or viral RNA synthesis in PCBP2-depleted cells (Figures 7F–7H). We conclude that miR-122 promotes new viral RNA synthesis, at least in part, by displacing PCBP2 from the viral RNA, decreasing the

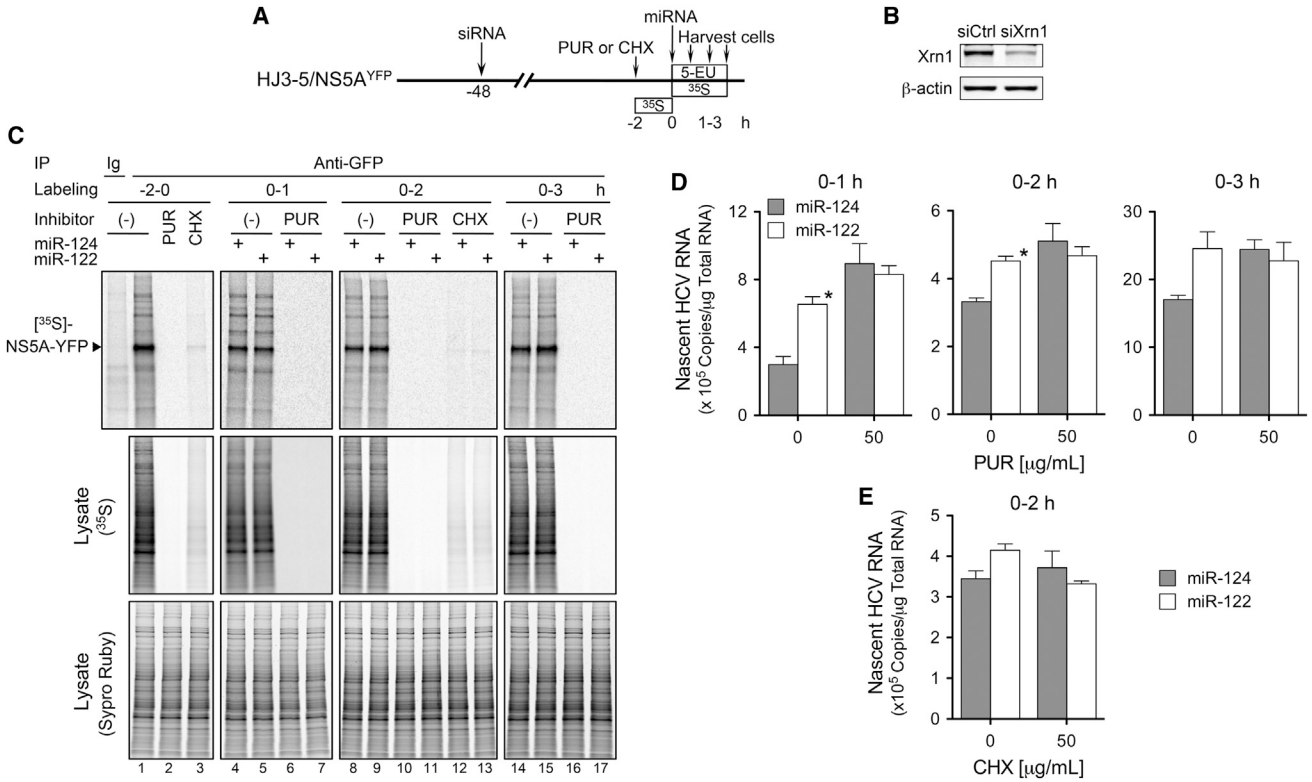

Figure 5. miR-122 Supplementation and Nascent HCV RNA following Short-Term Shutdown of Cellular Protein Synthesis

(A) Experimental design; HJ3–5/NS5A^{YFP} virus-infected cells were transfected with siRNAs, and then treated 2 days later with 50 μg/ml puromycin or cycloheximide for 2 hr prior to transfection of duplex miR-124 or miR-122 (0 hr). Following transfection of the miRNAs, cells were immediately fed with fresh media containing 5-EU or [^{35}S]-methionine/cysteine plus puromycin or cycloheximde for an additional 1–3 hr, then harvested for analysis of nascent viral RNA and protein.

(B) Immunoblot of Xrn1 48 hr after siRNA transfection. β-actin is a loading control.

(C) Protein synthesis following treatment with puromycin (PUR) or cycloheximide (CHX). Cell lysates collected after various labeling periods were immunoprecipitated with anti-GFP or isotype control (Ig) antibody, and the precipitates separated by SDS-PAGE. Radiolabeled proteins were visualized with a phosphorimager (top and middle panels). Total protein expression was determined by Sypro Ruby staining (bottom panel). Results shown are representative of multiple experiments.

(D) HCV RNA synthesis following shutdown of cellular translation. Total RNA was extracted from cells treated with puromycin at the times indicated, and 5-EU-labeled HCV RNA quantified as described in Experimental Procedures.

(E) HCV RNA synthesis 2 hr after shutdown of cellular translation with cycloheximide (CHX). Results shown in (D) and (E) represent the mean quantity of nascent viral RNA/μg total cellular RNA ± SEM in triplicate cultures, and are representative of multiple independent experiments. *$p < 0.05$ by two-way ANOVA. See also Figures S3 and S4.

fraction of viral RNAs engaged in translation and proportionally increasing the fraction available to template viral RNA synthesis.

DISCUSSION

Although miR-122 was found to be an important host factor for HCV almost a decade ago (Jopling et al., 2005), an understanding of its role in the viral life cycle has remained elusive. Our previous work indicates that the binding of miR-122 to two sites near the 5′ end of the viral genome stabilizes the RNA and protects it within infected cells from 5′ Xrn1-mediated decay (Li et al., 2013b; Shimakami et al., 2012a). Although a recent report suggested that Xrn2, a predominantly nuclear 5′ exonuclease, mediates HCV RNA decay (Sedano and Sarnow, 2014), we were unable to demonstrate this experimentally (Figure S1D). Importantly, we confirmed that miR-122 no longer influences the stability of HJ3–5 RNA in Xrn1-depleted cells (Figure S1F). Moreover, miR-122 supplementation increased the abundance of previously synthesized nascent RNA detected in control cells, but not in Xrn1-depleted cells (Figure S2). Collectively, these data provide strong justification for our use of Xrn1-depleted cells in the experiments described here.

While supplementing infected cells with exogenous miR-122 enhances the expression of HCV proteins (Jangra et al., 2010), the extent to which this results from a direct effect of miR-122 on the viral IRES or is secondary to stabilization of the genome or increased genome synthesis has been unresolved (Conrad et al., 2013; Henke et al., 2008; Roberts et al., 2011; Shimakami et al., 2012a). By developing methods allowing a direct comparison of the influence of miR-122 on viral RNA synthesis versus the synthesis of an essential viral nonstructural protein, NS5A, we have been able to show that transfection of duplex miR-122 induces significant increases in viral RNA synthesis in Xrn1-depleted cells prior to any increase in viral protein synthesis

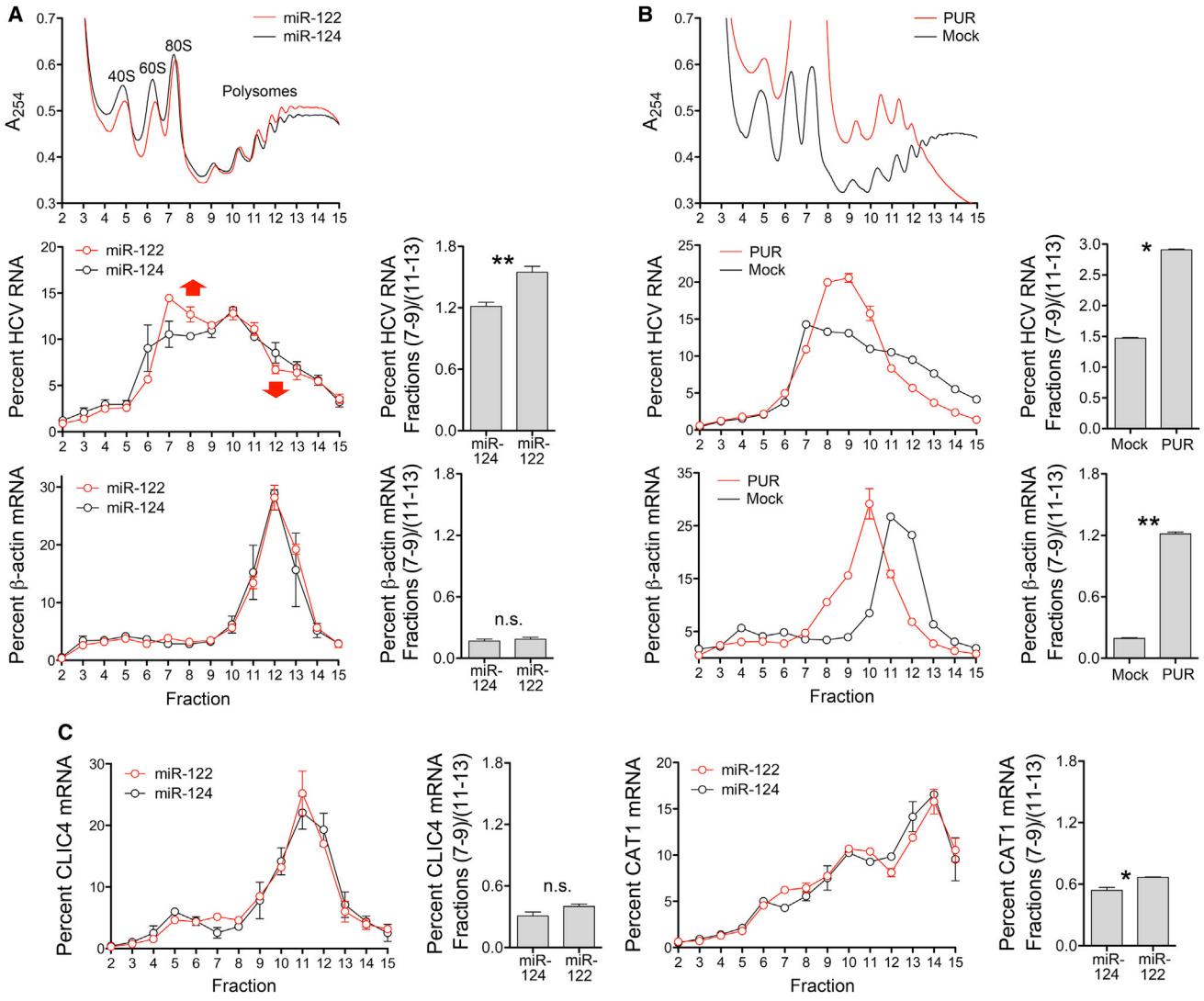

Figure 6. Polysome Analysis of Lysates from Infected, Xrn1-Depleted Cells Supplemented with miRNAs or Treated with Puromycin

(A) HCV-infected cells were harvested for polysome analysis (see Supplemental Experimental Procedures) following depletion of Xrn1 and transfection with miR-122 (red) or miR-124 (black) for 1 or 2 hr as outlined schematically in Figure 2A. Graphs on the left, from top to bottom, represent A_{254} and the distribution of HCV RNA and β-actin mRNA across 16 gradient fractions. RNA results are mean ± SEM percent of the total of that RNA in gradients from two independent experiments where cells were harvested 1 hr after miRNA transfection. On the right is the ratio of the cumulative percent RNA in fractions 7–9 divided by that in fractions 11–13 (polysomes) in gradients of lysates collected 1–2 hr after supplementation with miR-122 or miR-124. Results shown represent the mean ± SEM from three gradients in three independent experiments.

(B) Polysome analysis of lysates from cells treated for 3 hr with puromycin (PUR) 50 μg/ml (no miRNA supplementation). Release of RNAs from polysomes is only partial: lysates were not exposed to high-salt conditions prior to centrifugation, as the intent was to reflect conditions in the puromycin-treated cells shown in Figure 5. On the right is shown the ratio of percent HCV RNA and actin mRNA in fractions 7–9, divided by the percent in fractions 11–13 (polysomes) in the gradients shown on the left.

(C) Similar polysome analyses of CLIC4 and CAT1 mRNA in lysates collected 1 hr after transfection of miR-122 or miR-124. For all panels *$p < 0.05$, **$p < 0.01$ by two-sided paired t test; n.s., not significant. See also Figures S5 and S6.

(Figure 2D). These data provide strong evidence that miR-122 acts to directly promote HCV RNA synthesis, and that this leads to secondary increases in viral protein synthesis with subsequent expansion of viral replication complexes.

Kinetic analyses of increases in viral RNA and protein abundance following transfection of miR-122 in Xrn1-depleted cells indicated that there is very tight coupling of HCV translation and RNA replication (Figures 1C–1E). With some positive-strand RNA viruses, continued protein translation is required for ongoing synthesis of viral RNAs. For example, poliovirus RNA synthesis is dependent on translational activity of the viral RNA (Novak and Kirkegaard, 1994), and continuous protein synthesis is required for RNA synthesis by the coronavirus mouse hepatitis virus (Hagemeijer et al., 2012; Shi et al., 1999). Previous data suggest this is not the case for flaviviruses, including HCV (Shi et al., 2003; Westaway et al., 1999). We confirm this here

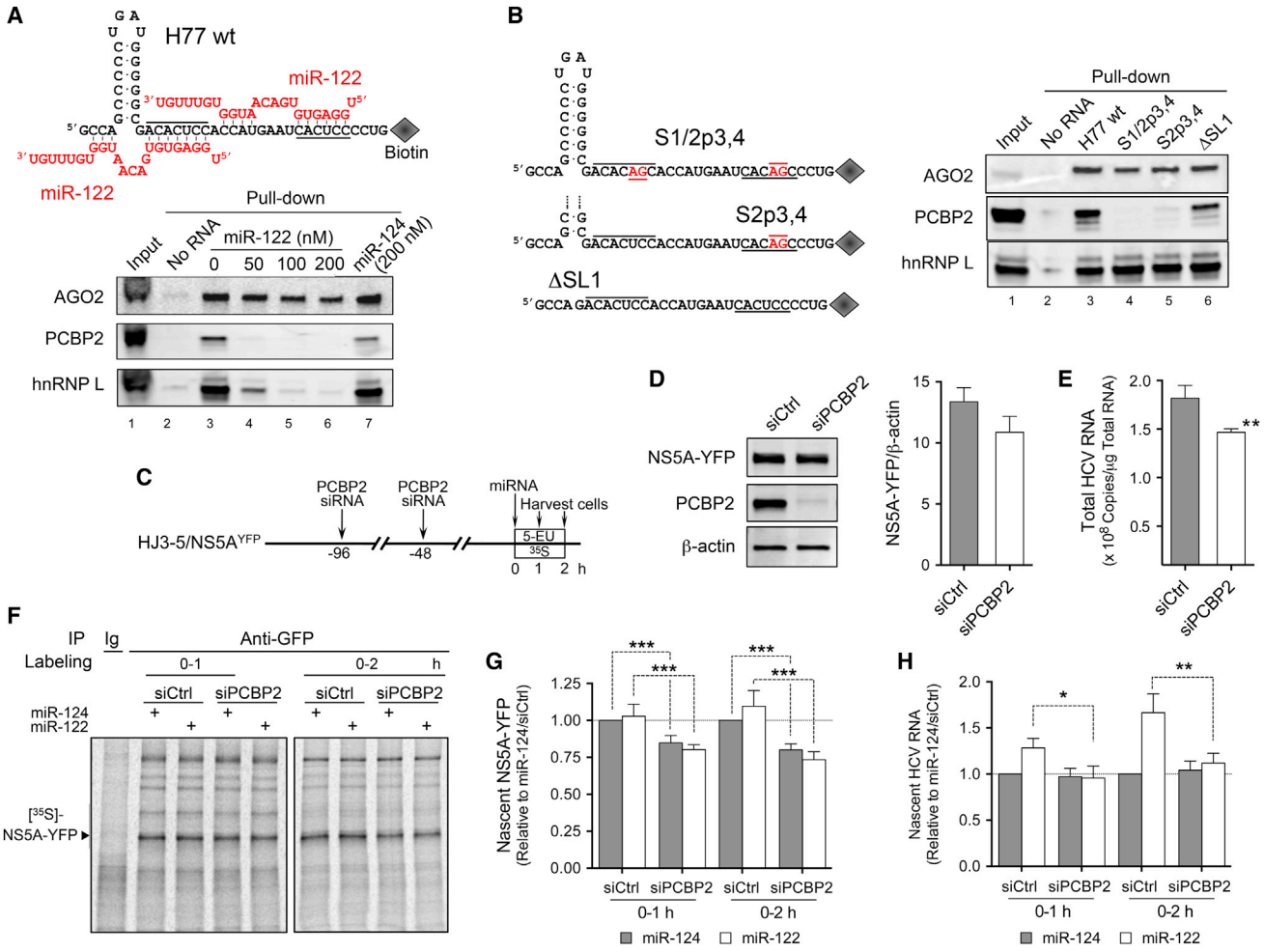

Figure 7. miR-122 Supplementation Does Not Stimulate RNA Synthesis in PCBP2-Depleted Cells

(A) Top: biotin-conjugated wild-type (wt) RNA bait representing the 5′ 47 nts of H77 HCV (Li et al., 2014). Two miR-122 molecules (red font) are shown bound to the bait (Jopling et al., 2008; Shimakami et al., 2012b). Seed sequence-binding sites are highlighted. Bottom: immunoblots of AGO2, PCBP2, and hnRNP L co-precipitating with the bait in a pull-down experiment. PCBP2 pull-down is eliminated by pre-annealing the bait with single-stranded miR-122 (but not miR-124). Input, Huh-7 cell lysate.

(B) Left: mutant RNA baits. Right: immunoblots of AGO2, PCBP2, and hnRNP L co-precipitating with the indicated bait.

(C) Design of experiments to assess impact of PCBP2 depletion on miR-122 stimulation of RNA synthesis. Stably infected cells were transfected twice with PCBP2-specific (siPCBP2) or control siRNA (siCtrl) prior to labeling with 5-EU and [^{35}S] as in Figure 2A. The cells were not depleted of Xrn1.

(D) Left: immunoblots of NS5A-YFP and PCBP2 in lysates of cells at time of harvest. β-actin was a loading control. Right: quantitative immunoblot analysis. NS5A-YFP abundance, normalized to β-actin, in siPCBP2-transfected cells was 83% ± 7% that in siCtrl-transfected cells (mean ± SEM, n = 4, p = 0.12 by Mann-Whitney test).

(E) HCV RNA abundance in lysates of cells at time of harvest. RNA abundance in siPCPB2-transfected cells was 80% ± 4% of siCtrl-transfected cells in two independent experiments, each involving three technical replicates. **p < 0.01 by Mann-Whitney test.

(F) NS5A-YFP synthesized following miRNA supplementation of PCBP2-depleted versus control cells. Cell lysates collected after 1- or 2-hr labeling were immunoprecipitated with anti-GFP or isotype control (Ig) antibody, and the precipitates separated by SDS-PAGE. Radiolabeled proteins were visualized with a phosphorimager.

(G) Phosphorimager quantitation of [^{35}S]-labeled nascent NS5A-YFP following miR-122 (open bar) or miR-124 (shaded bar) supplementation of PCBP2-depleted versus control cells with a 1- or 2-hr labeling period. NS5A-YFP synthesis was significantly dependent upon PCBP2 depletion, but not miR-122 supplementation (p < 0.0001 and p = 0.84, respectively, by two-way ANOVA).

(H) Nascent HCV RNA synthesis under the conditions described in (G). Nascent RNA synthesis was significantly dependent upon both PCBP2 depletion and miR-122 supplementation (p = 0.02 and p < 0.01, respectively, by two-way ANOVA). For both (G) and (H), results have been normalized to miR-124-transfected control (siCtrl-transfected) cells, and represent the mean ± SEM from five to six biological replicates in two independent experiments. *p < 0.05, **p < 0.01, ***p < 0.001 by ANOVA with Fisher's individual least significant difference test.

(Figure 5D). Surprisingly, however, our results show that active protein translation is required for miR-122 to stimulate nascent HCV RNA synthesis.

Based on studies with other positive-strand viruses, we recently speculated that miR-122 could promote HCV RNA synthesis by forming a complex that acts as a promoter for the viral

RdRp, or that might facilitate a requirement for cyclization of the genome prior to negative-strand RNA synthesis (Li et al., 2013a). We also considered the possibility that a miR-122 complex could stimulate new positive-strand RNA synthesis by binding the 5′ end of the positive-strand component of duplex replication intermediates, thereby promoting strand separation and freeing the 3′ end of negative-strand RNA to serve as template for new positive-strand RNA synthesis (Li et al., 2013a). While these remain possibilities, none of these hypotheses accounts for why active protein translation is required for miR-122 to stimulate RNA synthesis.

An alternative hypothesis that could explain the inability of miR-122 to stimulate viral RNA synthesis following shutdown of cellular translation is suggested by the need to regulate the engagement of viral RNA in translation versus RNA synthesis during positive-strand RNA virus replication. Since the genomes of these viruses serve as template for both translation and RNA synthesis, there is a conflict inherent in the 5′-to-3′ movement of translating ribosomes and the 3′-to-5′ translocation of the RdRp during negative-strand synthesis (Gamarnik and Andino, 1998). In the case of poliovirus, translation dominates until the viral protease becomes sufficiently abundant to cleave PCBP2, which binds the 5′ end of poliovirus RNA and in its intact form promotes IRES-directed translation (Perera et al., 2007). How HCV regulates the engagement of genomes in translation versus RNA synthesis is not known, but it is unlikely to utilize such an "on-off" switch due to the need to maintain continuous low-level replication in persistently infected hepatocytes. Puromycin acts to release translating ribosomes from messenger RNAs, thereby terminating translation. Similar to previous in vitro studies of poliovirus replication (Barton et al., 1999), puromycin-induced release of ribosomes from HCV RNA correlated in the short term with increased viral RNA synthesis (Figure 5D). In effect, puromycin induces an artificial switch from translation to replication.

miR-122 appears to act in a fashion similar to puromycin, facilitating a shift in the balance of HCV genomes engaged in translation versus RNA synthesis. The polysome analysis in Figure 6A shows that miR-122-induced increases in viral RNA synthesis are associated with a reproducible shift of viral RNAs from polysomes to the monosome fraction. This explains why miR-122 has no effect on RNA synthesis in the presence of puromycin, when all ribosomes have been released from the RNA, or following CHX treatment, when they are frozen in place. The miR-122 effect is only partial; substantial HCV RNA remains bound to polysomes and continues to be translated in the presence of miR-122 (Li et al., 2013a). However, miR-122 increases the fraction of RNA genomes available to template new RNA synthesis. It seems likely that miR-122 accomplishes this, at least in part, by displacing PCBP2 from the viral RNA (Figure 7) (Li et al., 2014). This may reduce the cyclization state of the viral RNA (Wang et al., 2011), potentially freeing 3′ UTR sequences for interactions with the replicase. Additional mechanisms may also be involved, including changes in the tertiary structure of the viral IRES (Mortimer and Doudna, 2013). The AGO2 complex recruited to HCV RNA by miR-122 could also function to reduce translation, as miRNA-induced silencing complexes normally do. Further efforts will be required to answer these questions, and to learn whether miR-122 promotes negative-strand or positive-strand viral RNA synthesis. However, the data presented here reveal a mechanism by which a miRNA regulates replication of a positive-strand virus by modulating the binding of cellular proteins to the viral RNA and controlling the balance between engagement of the RNA in protein translation versus viral RNA synthesis.

EXPERIMENTAL PROCEDURES

Cells and Reagents

Huh-7, Huh-7.5, and FT3–7 cells were maintained as described (Jangra et al., 2010; Shimakami et al., 2011). PSI-6130 (β-D-2′-deoxy-2′-fluoro-2′-C-methylcytidine) (Stuyver et al., 2006) and SOF (2′-deoxy-2′-α-fluoro-β-C-methyluridine-5′-monophosphate) (Murakami et al., 2010) were kindly provided by Angela Lam (Pharmasset, Princeton) and Ann Sluder (Scynexis, Research Triangle Park). Final dilutions contained 0.5% DMSO. CHX and puromycin were from Sigma-Aldrich (St. Louis) and InvivoGen (San Diego), respectively.

Virus Infections

HCV infections were initiated by electroporation of cells with RNA transcribed in vitro from a molecular clone, pHJ3–5, and (as a control) its replication-defective variant, pHJ3–5/GND (Yi et al., 2009). pHJ3–5/Gluc2A contains an in-frame insertion of the *Gaussia princeps* luciferase (GLuc) sequence between p7 and NS2 (Shimakami et al., 2011). pHJ3–5/NS5A^{YFP} is a related plasmid in which the enhanced YFP sequence has been inserted in-frame within the NS5A protein-coding sequence (Ma et al., 2011). In vitro transcribed RNA was electroporated into 5 × 10^6 Huh-7, Huh-7.5, or FT3–7 cells as described below. FT3–7 cells were cultured until more than 80% of cells were positive for core antigen expression by immunofluorescence assay. YFP-expressing Huh-7 cells were sorted by flow cytometry until nearly 100% of the cells were stably YFP positive.

RNA Oligonucleotides

Mature miRNA duplexes were generated by annealing equimolar amounts of guide and passenger strands. miR-122 and miR-124 were always transfected as duplexes, while anti-miR-122 and anti-random were transfected as single-stranded oligonucleotides. Sources and sequences of oligonucleotides are described in the Supplemental Experimental Procedures.

In Vitro RNA Transcription and Transfection

RNA transcripts were synthesized in vitro as described (Shimakami et al., 2011). For transfection, 5–10 μg RNA was mixed with 5 × 10^6 cells in a 4-mm cuvette and pulsed once at 250 V, 950 μF, and 50 Ω in a Gene Pulser Xcell Total System (Bio-Rad, Hercules). miRNA duplexes (50 nM), single-stranded oligonucleotides (50 nM), or siRNAs (20 nM) were transfected into cells using Lipofectamine RNAiMAX (Life Technologies, Carlsbad) according to the manufacturer's recommended procedures.

Immunoblots

Immunoblotting was carried out using standard methods with primary and IRDye-conjugated secondary antibodies (described in the Supplemental Experimental Procedures). Protein bands were visualized and quantified by densitometry with an Odyssey Infrared Imaging System (Li-Cor Biosciences, Lincoln).

HCV 5′ UTR-Protein Interactions

Biotin-conjugated RNAs representing the 5′ 47 nts of the HCV genome were chemically synthesized and used in pull-down experiments with hepatoma cell lysates as described previously (Li et al., 2014).

Quantification of miR-122 Co-Immunoprecipitating with AGO2

Cells were lysed in buffer containing 25 mM Tris-HCl (pH 7.4), 150 mM KCl, 5 mM EDTA, 1% Triton X-100, 5 mM dithiothreitol, protease inhibitor cocktail (Roche), and 100 U/ml RNaseOUT (Life Technologies). Lysates were precleared with 20 μl of Protein G Sepharose beads (GE Healthcare) for 1 hr at 4°C, then incubated with mouse monoclonal anti-AGO2 (MBL International) or isotype control IgG at 4°C for 2 hr, followed by addition of 20 μl of Protein

G Sepharose beads for 1 hr. Sepharose beads were washed six times in lysis buffer, and total RNA extracted using the miRCURY RNA Isolation Kit (Exiqon). miR-122 was quantified using the miRCURY LNA Universal RT microRNA PCR system and hsa-miR-122-5p LNA PCR primer set (Exiqon).

Metabolic Labeling and Measurement of Nascent HCV RNA and Protein Synthesis

Nascent RNA transcripts were quantified using the Click-iT Nascent RNA Capture Kit (Life Technologies) with modifications to the manufacturer's protocol. Cells were pulsed with 0.5 mM 5-EU for 1 hr, 0.3 mM 5-EU for 2 hr, or 0.2 mM 5-EU for more than 3 hr to incorporate 5-EU into newly synthesized RNA. Cells were then washed with PBS, and total RNA extracted using the RNeasy Mini Kit (QIAGEN, Venlo). Total RNA 5 μg and 0.5 mM biotin azide were used in a copper-catalyzed click reaction to conjugate biotin to 5-EU-labeled RNA. Following precipitation, the RNA was dissolved in 50 μl of RNase-free water. Biotin-conjugated 5-EU-RNA was isolated from 3 μg total RNA on streptavidin magnetic beads and used as a template for reverse transcription. cDNA synthesis was primed with an HJ3–5-specific primer using the SuperScript III First-Strand Synthesis System (Life Technologies), followed by TaqMan qPCR analysis using iQ Supermix (Bio-Rad) (see Supplemental Experimental Procedures for additional details). Nascent HCV RNA abundance was normalized to the total RNA (3 μg) used to capture nascent RNA transcripts on streptavidin magnetic beads, and is expressed as "copies/μg total RNA."

For [^{35}S] labeling, cells were cultured in methionine- and cysteine-deficient DMEM (Life Technologies) for 2 hr prior to the addition of 200 μCi/well of Express Protein Labeling Mix (PerkinElmer, Waltham). After incubation for 1–12 hr, cells were washed with PBS and lysed with 500 μl/well of lysis buffer (20 mM Tris-HCl [pH 7.4] containing 150 mM NaCl, 1% Triton X-100, 0.05% SDS, and 10% glycerol) supplemented with 50 mM NaF, 5 mM Na_3VO_4, and complete protease inhibitor cocktail (Roche, Mannheim). Cells were disrupted by 20 passages through a 25-gauge needle, and protein concentrations determined by Bradford Protein Assay (Bio-Rad). Lysates (130 μg total protein) were precleared with 10 μl of Protein G Agarose beads (Life Technologies) for 1 hr at 4°C, then incubated with rabbit anti-GFP or isotype control overnight at 4°C. Protein G Agarose beads (10 μl) were added to the lysate, incubated for 2 hr at 4°C, washed five times with 0.5 ml lysis buffer, then boiled for 5 min in 20 μl SDS sample buffer. Proteins were resolved by SDS-PAGE and visualized and quantified with a phosphorimager and ImageQuant software (GE Healthcare, Fairfield). To assess total protein synthesis, 10% of radiolabeled cell lysates were subjected to SDS-PAGE without immunoprecipitation. Proteins were directly visualized with Sypro Ruby Protein Gel Stain (Bio-Rad).

Polysome Profiling

3 × 10^6 HJ3–5/NS5A^{YFP}-infected Huh-7 cells in 10-cm dishes were treated with puromycin 50 μg/ml for 3 hr, or transfected with miRNAs and incubated for 1 or 2 hr. Cells were then incubated with CHX 100 μg/ml for 10 min, washed once with PBS containing CHX 100 μg/ml, and mechanically harvested. Cells were pelleted by low-speed centrifugation, resuspended in 1 ml polysome lysis buffer (PLB; 140 mM KCl, 5 mM $MgCl_2$, 20 mM Tris-HCl [pH 7.4], 0.01% Triton X-100, 10 mM DTT, 100 μg/ml CHX), then placed on ice for 10 min prior to passage through a 27-gauge needle five times before centrifugation at 1,000 × g. The resulting supernatant was clarified by centrifugation at 16,000 × g, then separated on a linear 10%–50% sucrose gradient prepared in PLB and centrifuged in an SW40 Ti rotor (Beckman, Brea) for 2 hr at 32,000 rpm at 4°C (no brake). A total of 16 fractions were collected from each gradient with continuous monitoring of absorbance at OD254 (UA-6; Isco, Lincoln). RNA was extracted from fractions using TRIzol reagent (Life Technologies) and subjected to cDNA synthesis with random primers, followed by qPCR quantitation of HCV, β-actin, CAT1, and CLIC4 cDNA (primer sequences are provided in Supplemental Experimental Procedures).

Statistical Analysis

Statistical comparisons were carried out by two-tailed Mann-Whitney test unless otherwise noted. Calculations were made with Prism 5.0c for Mac OS X software (GraphPad Software, La Jolla). $p < 0.05$ was considered significant.

SUPPLEMENTAL INFORMATION

Supplemental Information includes six figures and Supplemental Experimental Procedures and can be found with this article online at http://dx.doi.org/10.1016/j.chom.2014.12.014.

ACKNOWLEDGMENTS

We thank Angela Lam, Ann Sluder, and Charles Rice for reagents and antibodies. This work was supported in part by grants from the NIH, R01-AI095690 and R01-CA164029 (S.M.L.), R01-AI103311 (N.J.M.), T32-AI007419 (K.C.A.), and the University of North Carolina Cancer Research Fund. The UNC Flow Cytometry Core Facility is supported in part by National Cancer Institute grant P30-CA016086.

Received: June 14, 2014
Revised: September 16, 2014
Accepted: December 18, 2014
Published: February 5, 2015

REFERENCES

Barton, D.J., Morasco, B.J., and Flanegan, J.B. (1999). Translating ribosomes inhibit poliovirus negative-strand RNA synthesis. J. Virol. *73*, 10104–10112.

Chang, J., Nicolas, E., Marks, D., Sander, C., Lerro, A., Buendia, M.A., Xu, C., Mason, W.S., Moloshok, T., Bort, R., et al. (2004). miR-122, a mammalian liver-specific microRNA, is processed from hcr mRNA and may downregulate the high affinity cationic amino acid transporter CAT-1. RNA Biol. *1*, 106–113.

Conrad, K.D., Giering, F., Erfurth, C., Neumann, A., Fehr, C., Meister, G., and Niepmann, M. (2013). MicroRNA-122 dependent binding of Ago2 protein to hepatitis C virus RNA is associated with enhanced RNA stability and translation stimulation. PLoS ONE *8*, e56272.

Friebe, P., Lohmann, V., Krieger, N., and Bartenschlager, R. (2001). Sequences in the 5′ nontranslated region of hepatitis C virus required for RNA replication. J. Virol. *75*, 12047–12057.

Fukushi, S., Okada, M., Kageyama, T., Hoshino, F.B., Nagai, K., and Katayama, K. (2001). Interaction of poly(rC)-binding protein 2 with the 5′-terminal stem loop of the hepatitis C-virus genome. Virus Res. *73*, 67–79.

Gamarnik, A.V., and Andino, R. (1998). Switch from translation to RNA replication in a positive-stranded RNA virus. Genes Dev. *12*, 2293–2304.

Hagemeijer, M.C., Vonk, A.M., Monastyrska, I., Rottier, P.J., and de Haan, C.A. (2012). Visualizing coronavirus RNA synthesis in time by using click chemistry. J. Virol. *86*, 5808–5816.

Henke, J.I., Goergen, D., Zheng, J., Song, Y., Schüttler, C.G., Fehr, C., Jünemann, C., and Niepmann, M. (2008). microRNA-122 stimulates translation of hepatitis C virus RNA. EMBO J. *27*, 3300–3310.

Honda, M., Beard, M.R., Ping, L.H., and Lemon, S.M. (1999). A phylogenetically conserved stem-loop structure at the 5′ border of the internal ribosome entry site of hepatitis C virus is required for cap-independent viral translation. J. Virol. *73*, 1165–1174.

Jangra, R.K., Yi, M., and Lemon, S.M. (2010). Regulation of hepatitis C virus translation and infectious virus production by the microRNA miR-122. J. Virol. *84*, 6615–6625.

Janssen, H.L., Reesink, H.W., Lawitz, E.J., Zeuzem, S., Rodriguez-Torres, M., Patel, K., van der Meer, A.J., Patick, A.K., Chen, A., Zhou, Y., et al. (2013). Treatment of HCV infection by targeting microRNA. N. Engl. J. Med. *368*, 1685–1694.

Jopling, C.L., Yi, M., Lancaster, A.M., Lemon, S.M., and Sarnow, P. (2005). Modulation of hepatitis C virus RNA abundance by a liver-specific microRNA. Science *309*, 1577–1581.

Jopling, C.L., Schütz, S., and Sarnow, P. (2008). Position-dependent function for a tandem microRNA miR-122-binding site located in the hepatitis C virus RNA genome. Cell Host Microbe *4*, 77–85.

Kieft, J.S., Zhou, K., Jubin, R., and Doudna, J.A. (2001). Mechanism of ribosome recruitment by hepatitis C IRES RNA. RNA *7*, 194–206.

Lanford, R.E., Hildebrandt-Eriksen, E.S., Petri, A., Persson, R., Lindow, M., Munk, M.E., Kauppinen, S., and Ørum, H. (2010). Therapeutic silencing of microRNA-122 in primates with chronic hepatitis C virus infection. Science *327*, 198–201.

Li, Y., Masaki, T., and Lemon, S.M. (2013a). miR-122 and the hepatitis C RNA genome: more than just stability. RNA Biol. *10*, 919–923.

Li, Y., Masaki, T., Yamane, D., McGivern, D.R., and Lemon, S.M. (2013b). Competing and noncompeting activities of miR-122 and the 5′ exonuclease Xrn1 in regulation of hepatitis C virus replication. Proc. Natl. Acad. Sci. USA *110*, 1881–1886.

Li, Y., Masaki, T., Shimakami, T., and Lemon, S.M. (2014). hnRNP L and NF90 interact with hepatitis C virus 5′-terminal untranslated RNA and promote efficient replication. J. Virol. *88*, 7199–7209.

Ma, Y., Anantpadma, M., Timpe, J.M., Shanmugam, S., Singh, S.M., Lemon, S.M., and Yi, M. (2011). Hepatitis C virus NS2 protein serves as a scaffold for virus assembly by interacting with both structural and nonstructural proteins. J. Virol. *85*, 86–97.

Mortimer, S.A., and Doudna, J.A. (2013). Unconventional miR-122 binding stabilizes the HCV genome by forming a trimolecular RNA structure. Nucleic Acids Res. *41*, 4230–4240.

Murakami, E., Tolstykh, T., Bao, H., Niu, C., Steuer, H.M., Bao, D., Chang, W., Espiritu, C., Bansal, S., Lam, A.M., et al. (2010). Mechanism of activation of PSI-7851 and its diastereoisomer PSI-7977. J. Biol. Chem. *285*, 34337–34347.

Norman, K.L., and Sarnow, P. (2010). Modulation of hepatitis C virus RNA abundance and the isoprenoid biosynthesis pathway by microRNA miR-122 involves distinct mechanisms. J. Virol. *84*, 666–670.

Novak, J.E., and Kirkegaard, K. (1994). Coupling between genome translation and replication in an RNA virus. Genes Dev. *8*, 1726–1737.

Perera, R., Daijogo, S., Walter, B.L., Nguyen, J.H., and Semler, B.L. (2007). Cellular protein modification by poliovirus: the two faces of poly(rC)-binding protein. J. Virol. *81*, 8919–8932.

Pestova, T.V., Shatsky, I.N., Fletcher, S.P., Jackson, R.J., and Hellen, C.U. (1998). A prokaryotic-like mode of cytoplasmic eukaryotic ribosome binding to the initiation codon during internal translation initiation of hepatitis C and classical swine fever virus RNAs. Genes Dev. *12*, 67–83.

Pietschmann, T., Lohmann, V., Rutter, G., Kurpanek, K., and Bartenschlager, R. (2001). Characterization of cell lines carrying self-replicating hepatitis C virus RNAs. J. Virol. *75*, 1252–1264.

Roberts, A.P., Lewis, A.P., and Jopling, C.L. (2011). miR-122 activates hepatitis C virus translation by a specialized mechanism requiring particular RNA components. Nucleic Acids Res. *39*, 7716–7729.

Scheel, T.K., and Rice, C.M. (2013). Understanding the hepatitis C virus life cycle paves the way for highly effective therapies. Nat. Med. *19*, 837–849.

Sedano, C.D., and Sarnow, P. (2014). Hepatitis C virus subverts liver-specific miR-122 to protect the viral genome from exoribonuclease Xrn2. Cell Host Microbe *16*, 257–264.

Shi, S.T., Schiller, J.J., Kanjanahaluethai, A., Baker, S.C., Oh, J.W., and Lai, M.M. (1999). Colocalization and membrane association of murine hepatitis virus gene 1 products and de novo-synthesized viral RNA in infected cells. J. Virol. *73*, 5957–5969.

Shi, S.T., Lee, K.J., Aizaki, H., Hwang, S.B., and Lai, M.M. (2003). Hepatitis C virus RNA replication occurs on a detergent-resistant membrane that cofractionates with caveolin-2. J. Virol. *77*, 4160–4168.

Shimakami, T., Welsch, C., Yamane, D., McGivern, D.R., Yi, M., Zeuzem, S., and Lemon, S.M. (2011). Protease inhibitor-resistant hepatitis C virus mutants with reduced fitness from impaired production of infectious virus. Gastroenterology *140*, 667–675.

Shimakami, T., Yamane, D., Jangra, R.K., Kempf, B.J., Spaniel, C., Barton, D.J., and Lemon, S.M. (2012a). Stabilization of hepatitis C virus RNA by an Ago2-miR-122 complex. Proc. Natl. Acad. Sci. USA *109*, 941–946.

Shimakami, T., Yamane, D., Welsch, C., Hensley, L., Jangra, R.K., and Lemon, S.M. (2012b). Base pairing between hepatitis C virus RNA and microRNA 122 3′ of its seed sequence is essential for genome stabilization and production of infectious virus. J. Virol. *86*, 7372–7383.

Stuyver, L.J., McBrayer, T.R., Tharnish, P.M., Clark, J., Hollecker, L., Lostia, S., Nachman, T., Grier, J., Bennett, M.A., Xie, M.Y., et al. (2006). Inhibition of hepatitis C replicon RNA synthesis by beta-D-2′-deoxy-2′-fluoro-2′-C-methylcytidine: a specific inhibitor of hepatitis C virus replication. Antivir. Chem. Chemother. *17*, 79–87.

Thomas, D.L. (2013). Global control of hepatitis C: where challenge meets opportunity. Nat. Med. *19*, 850–858.

Wang, L., Jeng, K.S., and Lai, M.M. (2011). Poly(C)-binding protein 2 interacts with sequences required for viral replication in the hepatitis C virus (HCV) 5′ untranslated region and directs HCV RNA replication through circularizing the viral genome. J. Virol. *85*, 7954–7964.

Westaway, E.G., Khromykh, A.A., and Mackenzie, J.M. (1999). Nascent flavivirus RNA colocalized in situ with double-stranded RNA in stable replication complexes. Virology *258*, 108–117.

Yi, M., Ma, Y., Yates, J., and Lemon, S.M. (2009). Trans-complementation of an NS2 defect in a late step in hepatitis C virus (HCV) particle assembly and maturation. PLoS Pathog. *5*, e1000403.

Zhang, C., Huys, A., Thibault, P.A., and Wilson, J.A. (2012). Requirements for human Dicer and TRBP in microRNA-122 regulation of HCV translation and RNA abundance. Virology *433*, 479–488.